IEEE Access
Multidisciplinary | Rapid Review | Open Access Journal

Received 12 June 2022, accepted 23 June 2022, date of publication 29 June 2022, date of current version 5 July 2022.

Digital Object Identifier 10.1109/ACCESS.2022.3187111

RESEARCH ARTICLE

Performance Analysis of Random Access Mechanism in 5G Millimeter Wave Networks: Effect of Blockage, Shadowing and Mobility

LOKESH BOMMISETTY, (Member, IEEE), SAGAR PAWAR, AND T. G. VENKATESH
Department of Electrical Engineering, Indian Institute of Technology Madras, Chennai 600036, India
Corresponding author: Lokesh Bommisetty (lokesh.jun12@gmail.com)

This work was supported in part by the Prime Minister Research Fellowship, Ministry of Education, India.

ABSTRACT 5G NR has gained importance in academic and industrial research communities in recent times as its millimetre wave (mmWave) band operations offer a promising alternative for next-generation wireless communications. However, the susceptibility of mmWave signals to severe path loss and shadowing requires the use of highly directional antennas. Since the narrow beams are vulnerable to blockages, the interference behaviour becomes the key factor in building the network. In this paper, we propose a blockage model by considering the distribution of buildings in the cell as a Poisson point process. We analytically derive the blockage probability using the queuing theory. Subsequently, we derive the interference statistics using the blockage model considering the spatial randomness of the locations of blockages and User Equipments (UEs). We define and derive the coverage probability of a UE depending on the interference statistics. We calculate the success probability of a preamble transmission of a UE subjected its coverage. The effect of mobility on blockage, coverage and preamble success probability has been presented through extensive simulations.

INDEX TERMS 5G, blockage probability, performance evaluation, random access procedure, stochastic modelling.

I. INTRODUCTION

The explosive growth in the smart device market segment over the recent years has fueled a massive increase in the volume of the mobile data traffic. The wireless connectivity of smart devices has been growing exponentially in recent times [1]. 5G is a promising technology that enables massive machine type communications (mMTC) to address the growing device density and connectivity. 3GPP, in its Release 16, has defined two frequency ranges for operations which are FR1 band (Sub-6 GHz) and FR2 (millimetre wave) [2]. The Sub-6 band is already in use in LTE, which gives us a larger coverage area with low directionality.

Several studies in the literature have shown that the millimetre wave (mmWave) frequencies are suitable for cellular communication [3]. The system level performance of mmWave cellular networks is considerably superior to that of μWave networks, provided a sufficient beamforming gain is guaranteed between the base station (gNB) and the User Equipments (UEs) [3]. The use of mmWave in 5G NR is a key factor behind achieving higher throughput and supporting higher mobility speeds for UE. Nevertheless, the use of mmWave comes with its own limitations. The mmWave links are susceptible to blockage and have significant propagation path loss, which exhibits low probability of a Line-of-Sight (LoS) connection and unstable connectivity [4]. However, having larger antenna arrays that direct the radiation in desired directions will help to overcome the limitations of mmWave channels.

The highly directional links are extremely susceptible to obstacles in the cell region. The interference in such networks tend to exhibit an on-off pattern as a result of the movement of the UEs [5], [6]. Hence it is of utmost importance that the blockage characteristics of the links are

The associate editor coordinating the review of this manuscript and approving it for publication was Cunhua Pan.

to be studied in mmWave networks. The blockage characteristics give us the statistical understanding of whether a UE is in Line-of-Sight (LoS) or Non Line-of-Sight (NLoS) state. The path loss models for LoS and NLoS states of UE in mmWave operation are specified in the 5G NR standard [2]. Modelling the interference based on the blockage and path-loss models is crucial to set the right value of signal to interference and noise ratio (SINR) thresholds at the receivers.

In an urban setup, the UE often goes into the NLOS state due to the presence of obstacles. In NLOS state, beam pairs can still be formed via reflections and multi-paths. Nevertheless, as the UE moves through obstacles, the signal experiences propagation loss and shadow fading. This degradation in signal quality may lead to beam failure if the measured signal strength is below a specified threshold. If beam failure occurs, the UE has to initiate a random access procedure to re-establish connection with gNB. At each random access channel (RACH) instance, UE transmits a preamble selecting randomly from the set of available preambles in the cell to gNB. If the gNB is not able to detect the said preamble transmitted by UE, the RACH will be declared as failure and UE will initiate the RACH procedure again. Hence the number of UEs joining the network and their average joining time are affected by the success probability of the RACH procedure. Hence, it is important to analyse the performance of random access mechanism while considering the effect of blockage, outage and mobility.

The aim of the paper is to study the blockage and coverage performance of a UE using the path-loss models defined in the standard [2] and thus calculate the success probability of the RACH procedure. The major contributions of our paper are as follows.

- We model the obstacles as a Poisson point process (PPP) and derive the blockage probability of a UE using Poisson thinning and $M/G/1$ queuing methods.
- We incorporate the shadow fading and the path-loss models as per standard and derive the coverage probability of a UE.
- We simulate a realistic 5G NR environment, where UEs move according to a Gauss-Markov mobility model, to validate our analytical results.
- Through simulations, we show the effect of mobility on the performance of the blockage probability, coverage probability and the random access procedure.

The reminder of the paper is organised as follows. In section II, we present the related work. The network model is discussed in section III. We derive the blockage probability in section IV. The interference statistics and the coverage probability are derived in section V. The success probability of random access procedure is analytically derived in section VI. In section VII, we present and discuss the numerical results. In section VIII, we discuss the effect of mobility on the blockage probability, coverage probability and the RACH success probability using simulation results. The effect of self blockage on the NLoS probability and the random access of a UE is discussed in Section IX. We conclude the paper in section X.

II. RELATED WORK

The preliminary results showing the suitability of mmWaves for cellular communication have motivated the researchers to investigate the challenges and limitations of mmWave cellular communications [7], [8]. The interference modelling and system performance evaluation has been recognised to be an intractable problem due to the lack of models that realise the distribution on cellular users [9]. PPP is one of the popular models for the random distribution of nodes [10]. Mathematical flexibility of the PPP-based abstraction modelling has gained significance in developing analytical frameworks for evaluation of the system level performance of mmWave cellular networks [11]. The path-loss and blockage models in mmWave communications are significantly different from those of the μWave communications. Several works in the literature have modelled the blockage effect, assuming that the presence of one obstacle between the gNB and UE causes complete blockage of UE [12], [13]. However, it may take more than one obstacle to completely block the UE due to the beam width depending on the location of gNB, UE and the obstacle.

Di Renzo [11] have modelled the LoS and NLoS links and have pointed out that in mmWave communications, a new outage state is present in addition to the LoS and NLoS state, where the received signal strength at UE is below the desired threshold value. Vasanthan *et al.* have statistically modelled the hand blockage in mmWave cellular systems and have studies the implications of antenna placement in UE design [14], [15]. George *et al.* [16] have analysed the blockage performance of mmWave wearable networks where the users are considered to have a circular-shaped cross-section with finite radius. The propagation models and path loss models have been studied in [17], [18]. The working of beam pair formation has been studied in [19], [20]. Further, the study of the mobility of a UE in a given area is important to evaluate the blockage and coverage performance of a UE. Different mobility models such as the Manhattan model, Freeway model, Random Waypoint model have been studied in [21]. A recurrent Gaussian mobility model has been proposed in [22]. The model in [22] accurately represents the movement of a UE in a restricted area. This model has both temporal and spatial dependence, which is closer to the realistic movement of a UE. However, to the best of our knowledge, the study of how the mobility of an UE affects the beam failure, and how the obstacle densities in an area affects the beam failure has not been done extensively.

Unique features of our work are as follows.

- Unlike existing works [23], [24], we consider a realistic modelling of distribution and shapes of buildings to calculate the blockage probability of a UE.
- In contrast to [16], a novel queuing theory based approach is used for the first time to derive the blockage probability in our paper.

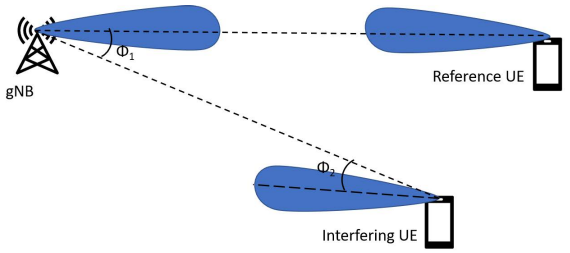

FIGURE 1. Illustration of the beam directions ϕ_1 and ϕ_2.

- To the best of our knowledge, ours is the first work to demonstrate the effect of obstacle density and mobility on the RACH success probability in presence of the shadowing effect.

We discuss the network model in the following section.

III. NETWORK MODEL

We consider a single base station with M number of UEs distributed in the cell uniformly. Obstacles are distributed according to a PPP with parameter γ [23], [25] and we consider a standard Friis path loss model for the communication [26]. We are interested in finding the interference statistics of a tagged UE and to calculate the success probability of the random access of the tagged UE. We assume that the base station (BS) is placed at the origin and the tagged UE is lying at a distance R_0. Let us denote $B_k(r)$ and S_k to be the random variables accounting for the blockage effect and the shadowing effect on k^{th} UE. $B_k(r)$ is a indicator random variable indicating whether the k^{th} UE located at a distance r is blocked from the basestation by an obstacle.

$$B_k(r) = \begin{cases} 1 & w.p \quad P_b(r) \\ 0 & otherwise \end{cases} \tag{1}$$

If $B_k(.)$ takes the value 1, it means that the UE is blocked and hence it is in NLoS state. UE in the LoS state is indicated by the random variable $B_k(.)$ taking the value 0. The probability of a UE located at a distance r from gNB being in NLoS state is given by $P_b(r)$. We analytically derive $P_b(r)$ in section IV. The practical propagation conditions are captured by the path-loss model with the path-loss exponents α_{LoS} and α_{NLoS} for LoS link and NLoS link respectively. In addition to the distance dependant path-loss model, each link is subjected to a random complex channel gain, which, for a generic gNB to UE link is denoted by h. According to [11], the shadow fading factor $S_k^s \sim |h|^2$ follows a log-normal distribution with mean μ_s and variance σ_s^2, where $s \in \{LoS, NLoS\}$ indicating the state of UE k. Let ϕ_1 be the azimuthal angle made by the line joining gNB and UE with the beam direction of gNB. Similarly, let ϕ_2 be the azimuthal angle made by the line joining gNB and UE with the beam direction of UE. A sample illustration of ϕ_1 and ϕ_2 is shown in Fig. 1 for a given interfering UE. Considering the above network model, the received power at the base station from the UE, k, located a distance r and in a state $s \in \{LoS, NLoS\}$ is given by

$$P_{R_X}^s(r, \phi_1, \phi_2) = P_{T_X} G_{max}^2 g(\phi_1) g(\phi_2) \left(\frac{\lambda}{4\pi r}\right)^{\alpha_s} S_k^s \tag{2}$$

where G_{max} is the maximum antenna gain, $g(\phi)$ is the normalised 2-Dimensional antenna gain pattern. P_{T_X} is the power transmitted by UE and $P_{R_X}^s$ is the corresponding received power at the base station. λ is the wavelength of the mmWave signal used for communication in the network. We consider a linear array of N flat-top antenna elements placed at $\lambda/2$ distance apart from each other. The gain pattern of the linear array antenna is given as [27]:

$$g(\phi) = \begin{cases} \frac{1}{N^2} \frac{sin^2(\frac{N}{2}\pi sin\phi)}{sin^2(\frac{1}{2}\pi sin\phi)}, & |\phi| \leq \frac{\theta}{2} \\ 0 & otherwise \end{cases} \tag{3}$$

where ϕ is the relative azimuth angle with respect to reference antenna and θ is the beam width. In consistence with the equation 2, the received power at the base station corresponding to the reference UE is $P_{R_X}^s(R_0, 0, 0)$ [24], [27]. Let us denote I_k to be the normalised interference power due to UE k experienced by the reference link. For the case of reference link in LoS and $NLoS$ state, the normalised interference is denoted as I_k^{LoS} and I_k^{NLoS} respectively and are given by the equations (4) and (5) respectively below. From I_k^{LoS} and I_k^{NLoS}, the normalised interference power without conditioning on the reference link state is given in (6).

$$I_k^{LoS} = \frac{P_{R_X}^{LoS}(r, \phi_1, \phi_2)(1 - B_k(r)) + P_{R_X}^{NLoS}(r, \phi_1, \phi_2) B_k(r)}{P_{R_X}^{LoS}(R_0, 0, 0)} \tag{4}$$

$$I_k^{NLoS} = \frac{P_{R_X}^{LoS}(r, \phi_1, \phi_2)(1 - B_k(r)) + P_{R_X}^{NLoS}(r, \phi_1, \phi_2) B_k(r)}{P_{R_X}^{NLoS}(R_0, 0, 0)} \tag{5}$$

$$I_k = (1 - B_0(R_0)) I_k^{LoS} + B_0(R_0) I_k^{NLoS} \tag{6}$$

A broad overview of the steps carried out in our analysis to derive the success probability of initial access on RACH is as follows.

- In Section IV, we model the length of arc at a given distance from the UE being blocked by any obstacle and the number of such arcs according to an M/G/1 queuing model and find the effective blocked length in equation (14).
- We then derive the average probability with which the tagged UE's LoS path being blocked due to the obstacles in equations (15) and (16).
- Using the blockage probability, we derive the coverage probability of a UE i.e., whether the received SINR at the UE is above a given threshold (equation (24)) in Section V. Hence, each UE is in the coverage region with the probability of P_{cov} given in (24).
- Tagged UE performs the initial access procedure in contention with the other UEs that are in the coverage region. The initial access procedure of the tagged UE

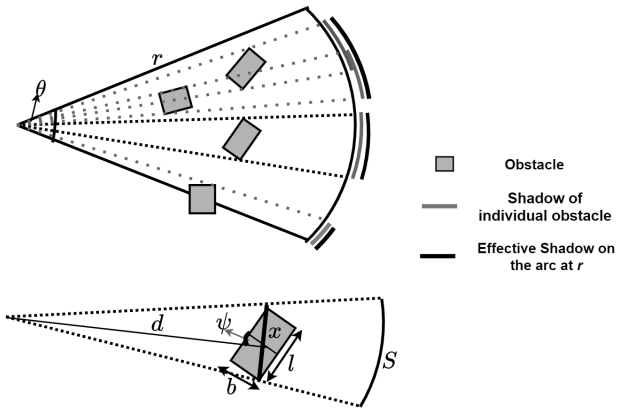

FIGURE 2. Blockage model.

is successful when no other contending UE transmits the same preamble that has been chosen by the tagged UE from the set of R preambles. Thus the expression for the success probability of RACH preamble transmission of a tagged UE is derived in Section VI and given in equation (27).

IV. BLOCKAGE PROBABILITY

In this section, we analytically derive the NLoS probability of a UE or the probability of a UE being blocked due to the obstacles present between the UE and the basestation. This analysis is of prime importance in 5G NR communication for the following reasons. Due to the high directionality of antenna patterns in 5G, the number of multipaths for a link will be limited. Besides, the high attenuation property of mmWave makes the reflected path signals weak. It is worth mentioning that in mmWave frequency communication, the LoS component dominates even the strongest NLoS component [23].

We consider the tagged UE to be located at a distance r from the base station. As discussed in the network model, the beam width is considered to be θ and the obstacles are distributed according to a PPP with parameter γ. Further, to closely model the obstacles (mainly buildings) in realistic scenario, we consider that the obstacles are rectangular shaped and also they can be in any orientation with respect to the LoS path of tagged UE. Fig. 2 shows a scenario of the obstructions seen by a UE located a distance r from the base station. The length l and breadth b of the obstacles are uniformly distributed in $[l_{min}, l_{max}]$ and $[b_{min}, b_{max}]$ respectively. Orientation of the obstacles is modelled by the random variable ψ, uniformly distributed in $[0, \pi]$ as shown in Fig. 2. Since the obstacles are distributed according to a PPP in the cell, the distribution of its distance d from the base station is given as

$$f(d) = \begin{cases} \dfrac{2d}{R^2} & 0 \le d \le R \\ 0 & otherwise \end{cases} \tag{7}$$

Let x be the projection length of the obstacle on the perpendicular bisector of the line joining the base station and the obstacle as shown in Fig. 2. The projection length, x can be written in terms of l, b and ψ as follows.

$$x = \begin{cases} l\cos(\psi) + b\sin(\psi) & 0 \le \psi \le \pi/2 \\ b\sin(\psi) - l\cos(\psi) & \pi/2 \le \psi \le \pi \end{cases} \tag{8}$$

Let S be length of the shadow created by the an obstacle on the arc located at a distance r from the base station (gray lines on the base of Fig. 2). For an obstacle located at a distance d from the base station, the shadow length is calculated as shown below.

$$S = r\arctan\left(\frac{x}{2d}\right) \tag{9}$$

where x is the projection of obstacle as given in (8). The expected shadow length $\mathbb{E}[S]$ is determined as follows.

$$\mathbb{E}[S] = \mathbb{E}_{d,l,b,\psi}\left[r\arctan\left(\frac{x}{2d}\right)\right] \approx \frac{2rk}{\pi R} \tag{10}$$

where

$$k = \left(\frac{l_{max}^2 - l_{min}^2}{2}\right)(b_{max} - b_{min}) + \left(\frac{b_{max}^2 - b_{min}^2}{2}\right)(l_{max} - l_{min}) \tag{11}$$

The effective shadowed length of the arc at a distance r from the basestation (black lines on the base of Fig. 2) is effectively the union of the individual shadows. Since the shadow lengths come from an uncountably infinite set (since the number of obstacles is given by Poisson distribution), the union of the individual shadows cannot be determined directly. The distribution of the number of individual shadows is PPP which is same as the number of blockages in the enclosed area of the sector shown in Fig. 2. The effective shadow is the overlapped individual shadows which can be considered as a thinned version of original PPP [23].

To calculate the effective shadow length, denoted by S_{eff}, we model the whole shadow projection process as an $M/G/\infty$ queuing system [28]. The justification of the $M/G/\infty$ modeling of the shadowing process is discussed as follows. The number of projections corresponds to the customer arrival according to Poisson distribution with parameter $\gamma\|\mathcal{A}\|$, where $\|\mathcal{A}\|$ is the area of the sector which is equal to $r^2\theta/2$. The projection length of each obstacle corresponds to its service time in the queuing system. We model the service time as a general process with the expected service time $\mathbb{E}[S]$ as given in equation (10). All the obstacles in the sector have projections at same time, equivalently can be said as the arrivals in the queue being served parallely, suggests an infinite server queuing system. Now, the effective shadow length can be determined as the duration for which the $M/G/\infty$ queue is non-empty in the time interval $[0, r\theta]$, total length of the arc. Using the steady state probabilities

of $M/G/\infty$, derived in [28], the effective shadow length is determined as

$$\mathbb{E}[S_{eff}] = (1 - exp(-\gamma \|\mathcal{A}\| \mathbb{E}[S]))\, r\theta \tag{14}$$

Since, the UEs are also distributed according to a PPP, the location of a UE given that it is at a distance r from basestation, is uniformly distributed over the circle of radius r. Hence the probability of the UE being blocked in a given sector is simply the ratio of the effective shadow length and the length of the arc in that sector.

$$\begin{aligned} P_b(r) &= \frac{\text{Effective shadow length}}{\text{length of the arc}} \\ &= (1 - exp(-\gamma \|\mathcal{A}\| \mathbb{E}[S])) \\ &= \left(1 - exp\left(-\frac{\gamma r^3 \theta k}{\pi R}\right)\right) \end{aligned} \tag{15}$$

Equation (15) shows the relation between the blockage probability of a UE with the system parameters γ, r, θ, k and R which is further discussed in detailed in Section VII Average blockage probability, P_b, of a random UE can be calculated by averaging (15) over the distribution of the distance of UE from the basestation.

$$\begin{aligned} P_b &= \mathbb{E}_r[P_b(r)] \\ &= \int_0^R (1 - exp(-\gamma \|\mathcal{A}\| \mathbb{E}[S]))\, \frac{2r}{R^2} dr \\ &= 1 + \frac{2}{3} E_{\frac{1}{3}}\left(\frac{\gamma \theta k R^3}{\pi R}\right) - \frac{2}{3R^2} \frac{\Gamma(\frac{2}{3})}{(\frac{\gamma \theta k}{\pi R})^{2/3}} \end{aligned} \tag{16}$$

where

$$E_n(x) = \int_1^\infty \frac{e^{-xt}}{t^n} dt.$$

V. INTERFERENCE STATISTICS AND THE COVERAGE PERFORMANCE

The normalised interference power caused by k^{th} UE, present at a location whose parameters are (r, ϕ_1, ϕ_2) to the reference link is given in (6). Given that the reference link is not blocked, the expected interference power due to k^{th} UE is given in equation (12), as shown at the bottom of the page.

As seen in equation (12), we have considered the cases where the k^{th} UE is in LoS condition and NLoS condition to calculate the expected interference power on the reference link due to k^{th} UE.

The terms $P_b(r)$ and $g(\phi)$ used in (12) are defined in equations (15) and (3) respectively. Let S_1 be the random variable defined by $S_1 \sim \frac{S_k^{LoS}}{S_0^{LoS}}$, the ratio of two i.i.d $lognormal(\mu_{LoS}, \sigma_{LoS}^2)$ random variables, and $f_{S_1}(s)$ is its probability distribution.

Theorem 1: Given $S_1 \sim \frac{S_k^{LoS}}{S_0^{LoS}}$, where $S_k^{LoS} \sim LN(\mu_{LoS}, \sigma_{LoS}^2)$ and $S_0^{LoS} \sim LN(\mu_{LoS}, \sigma_{LoS}^2)$, then

$$\mathbb{E}[S_1] = 1 + \frac{\sigma_{LoS}^2}{\mu_{LoS}^2}.$$

Proof: Proved in Appendix X-A. □

S_1 is a lognormal random variable with mean $1 + \frac{\sigma_{LoS}^2}{\mu_{LoS}^2}$ and variance $\left(1 + \frac{\sigma_{LoS}^2}{\mu_{LoS}^2}\right)^4 - \left(1 + \frac{\sigma_{LoS}^2}{\mu_{LoS}^2}\right)^2$. Similarly, let S_2 be the random variable defined by $S_2 \sim \frac{S_k^{NLoS}}{S_0^{LoS}}$. Hence, from (12), the expected value of the interference caused by a UE k with parameters (r, ϕ_1, ϕ_2) on an unblocked reference link can be completed using the following expressions.

$$\begin{aligned} \mathbb{E}[S_1] &= \int_0^\infty s f_{S_1}(s) ds = 1 + \frac{\sigma_{LoS}^2}{\mu_{LoS}^2} \\ \mathbb{E}[S_2] &= \int_0^\infty s f_{S_2}(s) ds = \frac{(\sigma_{LoS}^2 + \mu_{LoS}^2)\mu_{NLoS}}{\mu_{LoS}^3} \end{aligned} \tag{17}$$

Similarly, the expected normalised interference power due to UE k, when the reference link is in NLoS state is determined by the equation (13), as shown at the bottom of the page.

Let us define the random variables S_3 and S_4 such that $S_3 \sim \frac{S_k^{LoS}}{S_0^{NLoS}}$ and $S_4 \sim \frac{S_k^{NLoS}}{S_0^{NLoS}}$ respectively. From (13), the average interference caused by a UE k with parameters (r, ϕ_1, ϕ_2) on a reference link in *NLoS* state can be computed

$$\begin{aligned} \mathbb{E}\left[I_{k,(r,\phi_1,\phi_2)}^{LoS}\right] &= \mathbb{E}\left[g(\phi_1)g(\phi_2)\left(\frac{R_0}{r}\right)^{\alpha_{LoS}} \frac{S_k^{LoS}}{S_0^{LoS}}(1 - B_k(r))\right] + \mathbb{E}\left[g(\phi_1)g(\phi_2)\left(\frac{R_0^{\alpha_{LoS}}}{r^{\alpha_{NLoS}}}\right) \frac{S_k^{NLoS}}{S_0^{LoS}} B_k(r)\right] \\ &= P(B_k(r) = 0)\mathbb{E}\left[g(\phi_1)g(\phi_2)\left(\frac{R_0}{r}\right)^{\alpha_{LoS}} \frac{S_k^{LoS}}{S_0^{LoS}}\right] + P(B_k(r) = 1)\mathbb{E}\left[g(\phi_1)g(\phi_2)\left(\frac{R_0^{\alpha_{LoS}}}{r^{\alpha_{NLoS}}}\right) \frac{S_k^{NLoS}}{S_0^{LoS}}\right] \\ &= (1 - P_b(r))g(\phi_1)g(\phi_2)\left(\frac{R_0}{r}\right)^{\alpha_{LoS}} \mathbb{E}\left[\frac{S_k^{LoS}}{S_0^{LoS}}\right] + P_b(r)g(\phi_1)g(\phi_2)\left(\frac{R_0^{\alpha_{LoS}}}{r^{\alpha_{NLoS}}}\right) \mathbb{E}\left[\frac{S_k^{NLoS}}{S_0^{LoS}}\right] \end{aligned} \tag{12}$$

$$\mathbb{E}\left[I_{k,(r,\phi_1,\phi_2)}^{NLoS}\right] = (1 - P_b(r))g(\phi_1)g(\phi_2)\left(\frac{R_0^{\alpha_{NLoS}}}{r^{\alpha_{LoS}}}\right) \mathbb{E}\left[\frac{S_k^{LoS}}{S_0^{NLoS}}\right] + P_b(r)g(\phi_1)g(\phi_2)\left(\frac{R_0}{r}\right)^{\alpha_{NLoS}} \mathbb{E}\left[\frac{S_k^{NLoS}}{S_0^{NLoS}}\right] \tag{13}$$

by substituting the following expressions.

$$\mathbb{E}[S_3] = \int_0^\infty s f_{S_3}(s)ds = \frac{(\sigma^2_{NLoS} + \mu^2_{NLoS})\mu_{LoS}}{\mu^3_{NLoS}}$$
$$\mathbb{E}[S_4] = \int_0^\infty s f_{S_4}(s)ds = 1 + \frac{\sigma^2_{NLoS}}{\mu^2_{NLoS}} \quad (18)$$

Putting equations (12) and (13) together, we get the expectation of the normalised interference caused by the UE k whose parameters are (r, ϕ_1, ϕ_2) as follows.

$$\mathbb{E}[I_{k,(r,\phi_1,\phi_2)}] = P(B_0(R_0) = 0)\mathbb{E}\left[I^{LoS}_{k,(r,\phi_1,\phi_2)}\right] + P(B_0(R_0) = 1)\mathbb{E}\left[I^{NLoS}_{k,(r,\phi_1,\phi_2)}\right] \quad (19)$$

From (19), we calculate the average interference caused by any random UE in the cell by averaging it over the parameters r, ϕ_1 and ϕ_2 in equations (20), (21) and (22), as shown at the bottom of the page.

With the knowledge of the interference caused by a single UE, we now find the coverage probability of a given reference UE as follows. Since the locations of each UE and their blockage event in the cell is independent of the location of other UEs, the interference power caused by each UE is independent of the other i.e., $I'_k s$ are independent. According the physical model of interference, a UE is said to be in coverage zone of the basestation for its communication when the sum interference of the reference link is below a certain threshold $1/\beta$. With this definition, coverage probability of a UE in the presence of M interfering links can be mathematically written as

$$P_{cov} = P\left(\sum_{k=1}^{M} I_k \leq 1/\beta\right) \quad (23)$$

We apply the central limit theorem (CLT) to estimate $P(\sum_{k=1}^{M} I_k \leq 1/\beta)$. Conditioning that the reference link is unblocked, we have

$$P\left(\sum_{k=1}^{M} I_k \leq \frac{1}{\beta}\right) = 1 - Q\left(\frac{1/\beta - M\mathbb{E}[I_k]}{\sqrt{MVar(I_k)}}\right) \quad (24)$$

where $Q(\cdot)$ is the complementary cumulative distribution function for a standard normal distribution, given by $Q(x) = \frac{1}{2\pi}\int_x^\infty e^{\frac{-x^2}{2}}dx$ [29]. Substituting equation (24) in equation (23), we get the coverage probability of a UE denoted by P_{cov}.

VI. RACH SUCCESS PROBABILITY

In this section, we derive the success probability of preamble transmission of UE. For the connection establishment, every newly joining UE has to follow a random access procedure. Random access is a four step handshaking procedure between the UE and the gNB. In the first step of random access, all UEs transmit a preamble by randomly choosing from the available 64 preambles in its beam in the given PRACH slot. A UE will successfully finish its random access if the preamble chosen by it is not chosen by any other UE in that PRACH slot [30]. For the sake of generalisation, we consider that L preambles are available for the random access.

Let K be the random variable denoting the number of UEs other than the tagged UE which are in coverage range of gNB. The preambles transmitted by the UEs in coverage area only are detected at the gNB. The probability distribution of K can be expressed as follows.

$$P(K = k) = \binom{M}{k} P^k_{cov}(1 - P_{cov})^{M-k} \quad (25)$$

where M is the numbers of UEs served by the same beam other than the tagged UE. For a given UE to be successful, it should be in the coverage area and the rest of K UEs should choose a preamble different from that of the tagged UE. This can be mathematically written as follows.

$$P_s = \sum_{k=0}^{M} P(\text{tagged UE is covered})\left(1 - \frac{1}{R}\right)^k P(K = k) \quad (26)$$

By substituting (25) in (26), we get

$$P_s = \sum_{k=0}^{M} P_{cov}\left(1 - \frac{1}{L}\right)^k \frac{M!}{k!(M-k)!} P^k_{cov}(1 - P_{cov})^{M-k}$$

$$\mathbb{E}\left[I^{LoS}_k\right] = \mathbb{E}_{r,\phi_1,\phi_2}\left[\mathbb{E}[I^{LoS}_{k,(r,\phi_1,\phi_2)}]\right] = \iiint_{\phi_1,\phi_2=-\pi,r=0}^{\phi_1,\phi_2=\pi,r=R} \mathbb{E}[I^{LoS}_{k,(r,\phi_1,\phi_2)}]\frac{2r}{R^2}\frac{1}{4\pi^2}d\phi_1 d\phi_2 dr$$
$$= \frac{\theta^2}{2\pi}\frac{R_0^{\alpha_{LoS}}}{R^2}\left(\int_{r=0}^{R} \mathbb{E}[S_1]\frac{exp(-\gamma\|\mathcal{A}\|\mathbb{E}[S])r}{r^{\alpha_{LoS}}} + \mathbb{E}[S_2]\frac{1 - exp(-\gamma\|\mathcal{A}\|\mathbb{E}[S])r}{r^{\alpha_{NLoS}}}dr\right) \quad (20)$$

$$\mathbb{E}\left[I^{NLoS}_k\right] = \mathbb{E}_{r,\phi_1,\phi_2}\left[\mathbb{E}[I^{NLoS}_{k,(r,\phi_1,\phi_2)}]\right] = \iiint_{\phi_1,\phi_2=-\pi,r=0}^{\phi_1,\phi_2=\pi,r=R} \mathbb{E}[I^{NLoS}_{k,(r,\phi_1,\phi_2)}]\frac{2r}{R^2}\frac{1}{4\pi^2}d\phi_1 d\phi_2 dr$$
$$= \frac{\theta^2}{2\pi}\frac{R_0^{\alpha_{NLoS}}}{R^2}\left(\int_{r=0}^{R} \mathbb{E}[S_3]\frac{exp(-\gamma\|\mathcal{A}\|\mathbb{E}[S])r}{r^{\alpha_{LoS}}} + \mathbb{E}[S_4]\frac{1 - exp(-\gamma\|\mathcal{A}\|\mathbb{E}[S])r}{r^{\alpha_{NLoS}}}dr\right) \quad (21)$$

$$\mathbb{E}[I_k] = (1 - P_b(R_0))\mathbb{E}\left[I^{LoS}_k\right] + P_b(R_0)\mathbb{E}\left[I^{NLoS}_k\right] \quad (22)$$

$$= P_{cov}\left(P_{cov}\left(1-\frac{1}{L}\right)+(1-P_{cov})\right)^{M}$$
$$= P_{cov}\left(1-\frac{P_{cov}}{L}\right)^{M} \quad (27)$$

Equation (26) gives the average success probability of the preamble transmission of a UE.

VII. VALIDATION OF ANALYTICAL RESULTS

In this section, we present the numerical results obtained in Sections IV, V and VI to demonstrate the performance of the random access procedure as a function of different network parameters. We plot the analytical results numerically in MATLAB and validate them using the simulations performed using the 5G toolbox of MATLAB. For these simulations, we consider that the UEs are static. We assume that the shape factor of Nakagami distribution is set to 5. The beam width of mmWave signals is set to 20 degrees. The results are obtained for different values of obstacle densities (γ) and the number of UEs in the cell (M). We discuss the results for blockage probability, coverage probability and RACH success probability in the below subsections.

A. BLOCKAGE PROBABILITY

Blockage probability, as defined in Section IV, is the probability that a UE is in the NLoS state due to the presence of obstacles in the path of UE and gNB. In figures 3a and 3b we plot the blockage probability of a UE for different densities of obstacles distributed in the cell and the distance of UE from gNB. For a UE at a given distance from gNB, the blockage probability increases with the obstacle density and gets saturated to 1 as can be seen in equation (15). Further, the intuition for the behaviour of blockage probability is discussed as follows. Initially, in the lower range of γ, as the obstacles are sparse, the additional obstacles introduces in the cell will create a non overlapping shadow and hence the blockage probability increases sharply. But at higher values of γ, the new obstacles introduced in the cell will have their shadowed region overlapped with the existing shadow and hence have a little effect on the blockage probability. Hence, the rate of increase in the blockage probability decreases with γ and finally saturates.

It can be seen from Fig. 3b that the blockage probability saturates at lower values of γ with the increase in the distance between the UE and gNB. This is because, for a given γ, a UE at a greater distance is obstructed by more number of blockages when compared to the UE that is closer to gNB. Hence the fraction of the effective shadow length increases with r and therefore the blockage probability also increases with r. This can also be seen from equation (15) as follows. For a given γ in (15), the blockage probability increases exponentially with $\|\mathcal{A}\|\mathbb{E}[S]$, where $\|\mathcal{A}\| \propto r^2$ and $\mathbb{E}[S] \propto r$. Hence, the blockage probability grows exponentially with r^3 for a given γ which results in two turning points when blockage probability is plotted against r as shown in Fig. 3b before the curve saturates to 1.

B. COVERAGE PROBABILITY

In figures 4 and 5, we show the performance of the communication link between the UE and gNB in terms of the coverage probability that is derived in section V. In Fig. 4a, we plot the coverage probability of a UE against the threshold β for different values of obstacle density γ, when there are 200 interfering UEs in the beam direction. As expected from the equation (24), with the increase in threshold, the coverage probability of UE reduces as the coverage probability has the inverse relation with the Q-function in equation (24). With the increase in obstacle density (γ), initially the coverage probability reduces sharply due to the blockage of tagged UE as shown in Fig. 4b. This can be justified using Fig. 3a where we discussed the sharp increase in blockage probability in the initial range of γ as followed from equation (15). In the mid range of γ, the coverage probability improves with increase in γ as the interfering UEs also get blocked and hence SIR improves for the tagged link.

In Fig. 5, we show the performance of coverage probability with the number of interfering UEs in the beam direction as that of the tagged UE. In Fig. 5, we consider a log spaced values of M, the number of interferers, between 1 and 500 to capture the meaningful variation in the coverage performance. The coverage performance deteriorates with increase in M for a given $\gamma = 0.35$ as shown in Fig. 5a which is supported by equation (24) as Q-function increases with M. In Fig. 5b, it is shown that for all M, the coverage probability saturates to a same value of 0.394 when the obstacle density is high. However, in the moderate range of γ, the number of interfering UEs have a significant impact on the coverage probability. For example, for $\gamma = 0.6$, the coverage probability when $M = 5$ is 0.42 which is very high when compared to the case of $M = 500$, where the coverage probability is only 0.02.

C. SUCCESS PROBABILITY

In Fig. 6, we plot the success probability of UE for different values of the number of interferers (M) and obstacle density (γ). In these plots, we consider that the number of available preambles in $R = 64$. The success probability of the UE is the probability with which the preamble transmitted by UE is received at gNB and it is the unique. For a given M, the success probability decreases with the obstacle density monotonically when M is small. But for higher values of M, the trend of success probability against γ is not monotonic for the following reasons. The number of UEs which are in coverage zone is a binomial random variable as given by equation (25) which results in the coverage performance shown in Fig. 5b. Hence, in the initial range of γ, all UEs are almost in coverage range and hence contention is high when M is large, resulting in low success probability. With increase in γ, the number of UEs in coverage zone reduces and hence the contention reduces resulting in an improved success probability. With further increase in γ, as the coverage probability increase and gets saturated, success probability shows an inverse behaviour. For a given γ, the

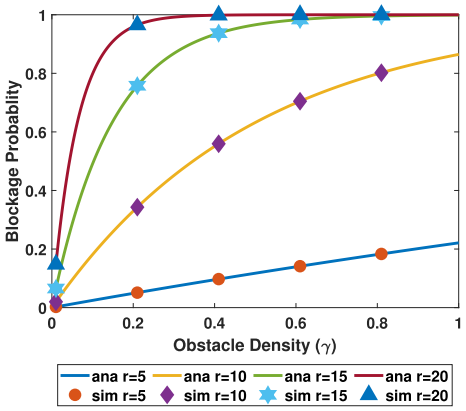

(a) Probability of blocking against the blockage density γ for a UE at a distance r

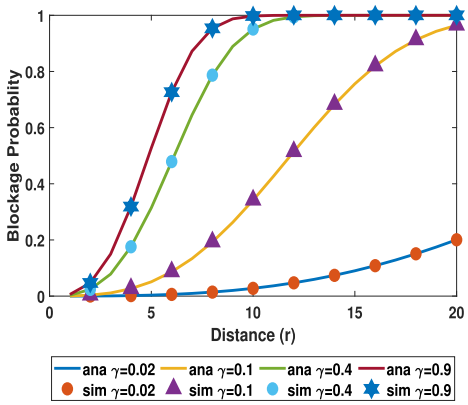

(b) Probability of blocking for a UE at a distance r for different blockage densities

FIGURE 3. **Probability of blockage or the NLoS probability.**

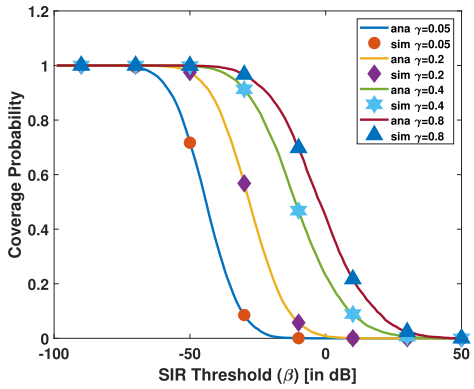

(a) Coverage Probability against the threshold (β) for different obstacle densities (γ)

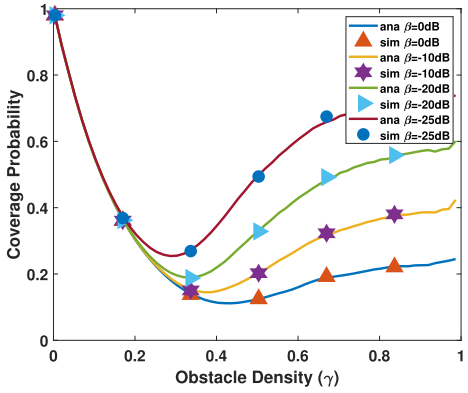

(b) Coverage Probability against the obstacle density (γ) for different threshold values(β)

FIGURE 4. **Coverage probability of a UE for the variations of SIR threshold (β) and the obstacle density (γ).**

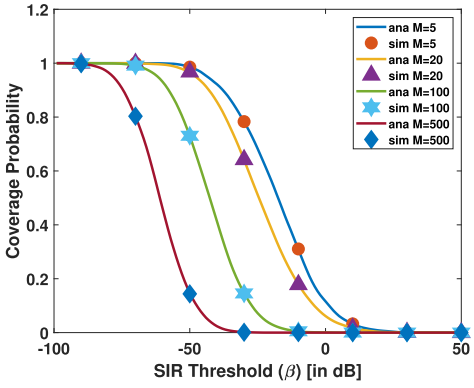

(a) Coverage Probability against the threshold (β) for different number of UEs (M)

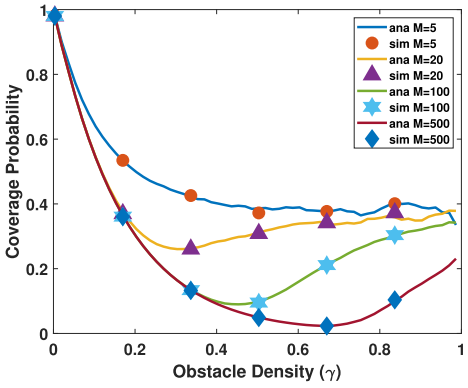

(b) Coverage Probability against the obstacle density (γ) for different number of UEs (M)

FIGURE 5. **Coverage probability of a UE for different number of UEs (M) in a beam direction.**

success probability of a UE decreases monotonically with the increase in number of UEs (M) as shown in Fig. 6b because of the increase in contention. This behavior of the random access success probability in Fig. 6 is expected from equation (27)

as the success probability is a binomial function of order M.

VIII. EFFECT OF MOBILITY ON RANDOM ACCESS PROCEDURE

We model the movement of UE in a restricted area with buildings as obstacles. Different mobility models have been considered for various scenarios such as Urban Macro (UMa), Urban Micro (UMi), Rural and indoor cases in [22]. We consider that the obstacles in the cell are stationary and the UEs move according to Gauss-Markov mobility model in the cell as explained below.

1) GAUSS-MARKOV MOBILITY MODEL

Gauss-Marokov mobility model has a temporal dependence which can mimic a random and continuous movement of an UE in open area. For our model we wish to restrict the mobility of UE in a given area hence we make a partial use of model defined in [22] which defines Gauss-Markov Mobility as follows:

$$\begin{aligned} S_{t+1} &= \alpha S_t + (1-\alpha)\overline{S} + \sqrt{1-\alpha^2}\mathcal{N}(0,1) \\ D_{t+1} &= \alpha D_t + (1-\alpha)\overline{D} + \sqrt{1-\alpha^2}\mathcal{N}(0,1) \end{aligned} \quad (28)$$

where S_{t+1} and D_{t+1} represent speed and direction at next instance, $\overline{S}$ and $\overline{D}$ are mean speed and direction, α is tuning parameter and $\mathcal{N}(0,1)$ is Standard Normal Random Variable. Based on (28) we define next position of UE as:

$$\begin{aligned} x_{t+1} &= x_t + S_{t+1}cos(D_{t+1}) \\ y_{t+1} &= y_t + S_{t+1}sin(D_{t+1}) \end{aligned} \quad (29)$$

Note that for $\alpha = 0$, the mobility model loses its dependence on previous speed (S_{t-1}) in (28). But in realistic scenario, the current speed (S_t) depends on the previous value of speed (S_{t-1}). When $\alpha = 1$, the speed and direction become constant, which is also undesirable considering the randomness in the realistic scenario.

We generate obstacles, such that the number of obstacles are generated using PPP and then obstacles are placed uniformly across the area near gNB. Fig.7 shows an example path traced by UE following the given mobility model. It mimics the continuous path that can be taken by a UE. Obstacles represent buildings in the area.

For simulation of UE mobility, we use the parameters given in Table 1. We consider a square area of dimensions 500 × 500 meters, in 2-D considering the top view of the area. gNB is located at the origin of the map. We consider a pedestrian/vehicular scenario, assumption being made that the UE is outside the buildings. All simulations have been done using MATLAB. Simulation is carried as follows.

- For each iteration, model the mobility of UE using (28) (29) for 10,000 instances and obstacles using PPP.
- For each instance, determine the status of UE i.e. unblocked or blocked (LOS or N-LOS) described in Section VIII-A

TABLE 1. Mobility parameters.

Parameters	Values
α	0.1 to 0.9
$\overline{S}$	1 to 10 m/s
S_t(initial speed)	$\mathcal{U}$[0,1]*$\overline{S}$
D_t(initial direction)	$\mathcal{U}$[0,2π]
x_t,y_t	$\mathcal{U}$[-250,250]
Length of buildings (l)	$\mathcal{U}$[10,30] meters
Breadth of buildings (b)	$\mathcal{U}$[10,30] meters
Location of buildings	$\mathcal{U}$[-250,250]
Number of Instances	10000

- Depending on the status of UE and find the path-loss for every instance described in Section VIII-B
- Simulate above steps for 1000 iterations to arrive at the P(N-LOS) and probability of beam failure.

A. BLOCKAGE PROBABILITY

For the blockage condition to occur, there must be no direct path from the position of UE to gNB. This can occur when the UE is behind a certain obstacle, with respect to gNB. Using Table 1 we choose the length and the breadth of each building to be uniformly distributed between 10 and 30 meters. Considering the quadrant in which an obstacle lies we decide two corner points and calculate their angles and distance from origin. If at any instance UE lies beyond the measured distance of obstacle and in between the angles, then the blockage is declared.

Fig.8a shows the blockage probability of a UE at any given instance in the cell. It is observed that by increasing the obstacle density, the blockage probability increase. The curve of blockage probability, on initial observations, may mimic the curve of $1 - \exp(-\beta x)$ and then saturates to 1 for the higher values of obstacle density (γ). This is expected, as the number of building are very high in the given area, the UE will tend to remain in shadowed region at any instance. This in turn, validates our system model. The effect of tuning parameter α and the mean speed $\overline{S}$, defined in VIII-1 is also observed in Fig 8a and 8b respectively. It is observed that varying the tuning parameter α in (28) from 0.1 to 0.9 does not affect the NLOS probability in any way. Thus the effect of α can be neglected. Similarly, the change in means speed also does not affect the blockage probability as shown in Fig. 8b.

B. COVERAGE PROBABILITY

In 5G NR, beam Failure may occur due to fast shadowing experienced by UE or while beam-switching. Beam Failure is essential to account for RACH procedure performance as RA occasion is triggered when beam failure occurs. For Beam-Failure to be declared following condition have to be satisfied:

- The path-loss experienced by UE at any instance in accordance with Table.3 defined in [2] should be greater than a set threshold value Ω.
- The UE should remain in above condition for two or more instances.

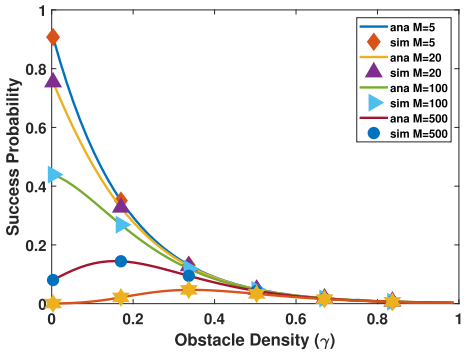

(a) RACH success probability against the obstacle density (γ) for different number of UEs (M)

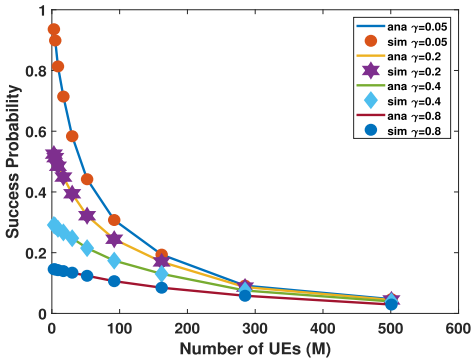

(b) RACH success probability against the number of UEs (M) for different values of obstacle density (γ)

FIGURE 6. Success Probability of the preamble transmission of a UE.

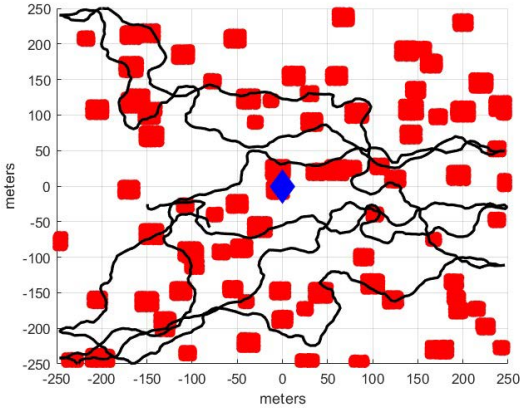

FIGURE 7. Example traces (black lines) of the path of UE (blue marker) based on the Gauss-Markov mobility model and PPP obstacle (red blocks) distribution model.

TABLE 2. Mobility parameters.

Variables	Values
h_{UT}	1.5 meters
h_{BS}	25 meters
f	30×10^9 Hz
f_c	30 GHz normalised with 1 GHz

TABLE 3. Path Loss model for Urban Macro-cellular (UMa) region.

LoS	$PL_{UMa-LOS} = \begin{cases} PL_1 \text{ for } 10m \le d_{2D} \le d'_{BP} \\ PL_2 \text{ for } d'_{BP} \le d_{2D} \le 5km \end{cases}$ $PL_1 = 28.0 + 22log_{10}(d_{3D}) + 20log_{10}(f_c)$ $PL_2 = 28.0 + 40log_{10}(d_{3D}) + 20log_{10}(f_c)$ $-9log_{10}[(d'_{BP})^2 + (h_{BS} - h_{UR})^2]$	$\sigma_{SF} = 4$
NLoS	$PL_{UMa-NLOS} = max(PL_{UMa-LOS}, PL'_{UMa-NLOS})$ $for\ 10m \le d_{2D} \le 5km$ $PL'_{UMa-NLOS} = 13.54 + 39.08log_{10}(d_{3D}) +$ $20log_{10}(f_c) - 0.6(h_{UT} - 1.5)$	$\sigma_{SF} = 6$

In Table.3, d_{2D} is the distance between the base of gNB to position of UE. d_{3D} is the distance of UE from antenna of gNB.h_{UT} and h_{BS} are height of UE and gNB respectively. σ_{SF} represents the standard deviation of shadow fading. When calculating path loss we also have to take into account the shadow fading of the channel in order to accurately estimate the total path loss.

$$d_{3D} = \sqrt{d_{2D}^2 + (h_{BS} - h_{UT})^2}, \quad 1.5m \le h_{UT} \le 22.5m \tag{30}$$

$$d_{BP} = \frac{4h_{BS}h_{UT}f}{c} \tag{31}$$

The values used for calculation for path loss from (30) (31) and Table. 3 are given in Table 2. Fig. 9a, 9b show the probability of coverage across obstacle density for different values of parameters α and $\overline{S}$. We observe in Fig. 9a that, for constant mean speed of $1ms^{-1}$, the coverage probability decreases with increase in obstacle density. Moreover, the coverage probability starts saturating around 65% higher obstacle density range i.e from 0.8 to 1. A key observation is that the coverage probability is independent of tuning parameter α.

In Fig. 9b, we keep $\alpha = 0.9$, and vary mean speed from $1ms^{-1}$ to $10ms^{-1}$. We observe that the coverage probability saturates around 65% for higher obstacle densities i.e from 0.8 to 1. For obstacle densities in the range 0 to 0.6 we observe that for lower mean speed values i.e., from $1ms^{-1}$ to $4ms^{-1}$, the coverage probability decreases monotonically, similar to the observations from Fig. 9a. And for higher mean speeds i.e., from $5ms^{-1}$ to $10ms^{-1}$, we observe that the coverage probability decreases rapidly up-to obstacle density of 0.2 and then increases to rise up-to the saturation point. We observe that higher the mean speed, the rate of decrease in coverage probability is higher for the range of obstacle density 0 to 0.2.

This trend can be attributed to the fact that, for lower to moderate obstacle densities i.e., from 0 to 0.5, as mean speed increases, the UE tends to switch from LOS to NLOS state more frequently and vice-versa. This increases the chance of UE going beyond the path loss threshold Ω for longer, thus counting towards lower coverage probability. For higher obstacle densities the $P(NLOS)$ is very high and UE tends to remain beyond path loss threshold Ω for a long periods of

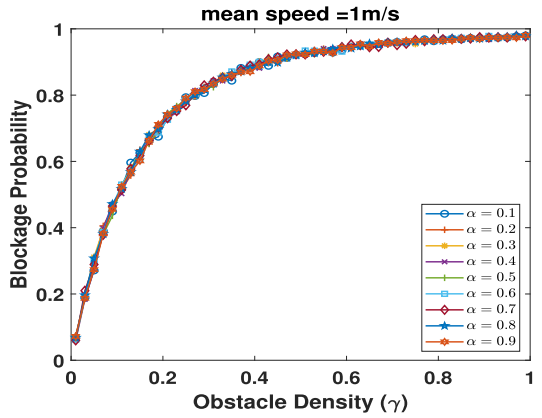

(a) Effect of Tuning Parameter (α) on Blockage

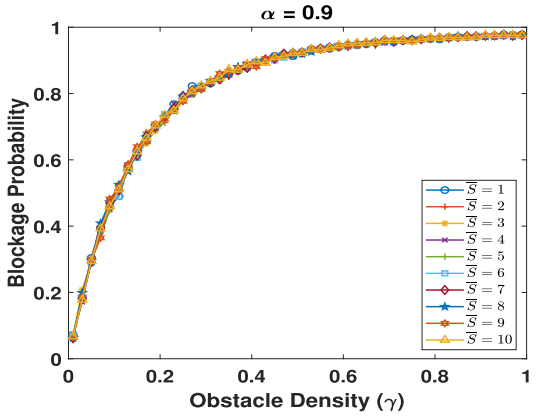

(b) Effect of mean speed ($\overline{S}$) on Blockage Probability

FIGURE 8. Effect of mobility on the blockage probability.

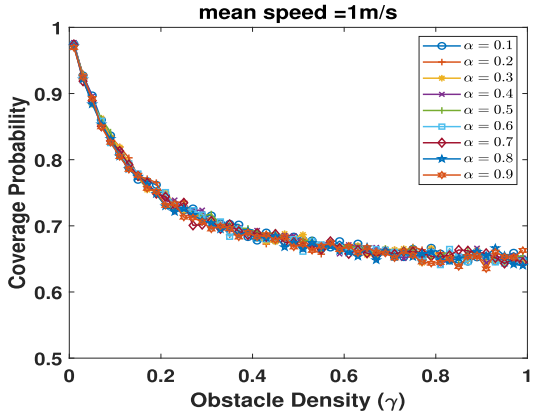

(a) Effect of Obstacle Density (γ) and α on coverage probability

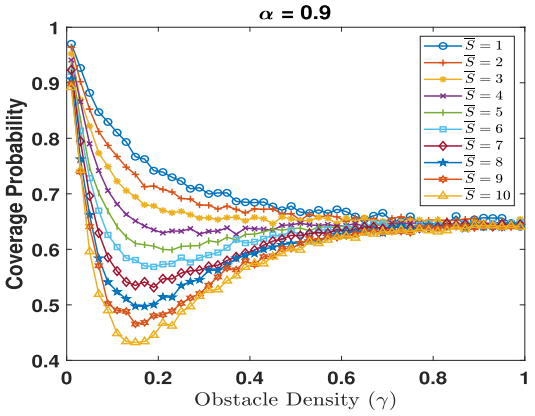

(b) Effect of Obstacle Density (γ) and Mean Speed $\{\overline{S}\}$ on coverage probability

FIGURE 9. Effect of α and $\overline{S}$ on the coverage probability of UE.

time, irrespective of the speed, thus saturating the coverage probability, independent of speed.

C. RACH SUCCESS PROBABILITY (P(SUCCESS))

We define RACH success probability $P(success)$ as the conditional probability that the transmitted preamble by an UE at any given instance, does not encounter collision, given that the preamble is detected at gNB.

For simulations, we consider a restricted area of $500m \times 500m$, with the movement of UE based on the Gauss-Markov mobility model. When a UE is not in the coverage zone, beam failure is declared and UE will loose connection to the gNB and the beam pair formation breaks. In order to initiate PRACH and transmit preamble, beam pair formation is required. As soon as the UE is in the region where signal power loss is above the threshold Ω, UE will form a beam-pair with gNB and initiate RACH. For initiating RACH, UE selects randomly any one of the 64 available preambles, and transmits it to gNB. If the preamble is detected at the gNB accurately we declare that RACH procedure is successful, with the assumption that the further signalling required for RACH procedure is successful. For multiple users, the preamble transmission may occur at same time, at this instance, all UEs in the area will transmit the preambles at same time which randomly selected from the same pool of 64 preambles. It may so happen that the same preamble is selected by multiple UEs and transmitted. If detected at gNB, this will cause a preamble collision and RACH failure will be declared.

In Fig. 10a, we observe that for lower number of users ($M = 5$), success probability decreases with increasing obstacle density and saturates around 25%. By varying mean speed from $1m/s$ to $9m/s$, it is observed that the success probability curve follows a similar trend as observed in Fig. 9b. As the number of UE transmitting are low and their position at any given instance are independent, the probability of multiple UEs being recovered from beam failure and transmitting the preamble at the same instance is very low. Thus,

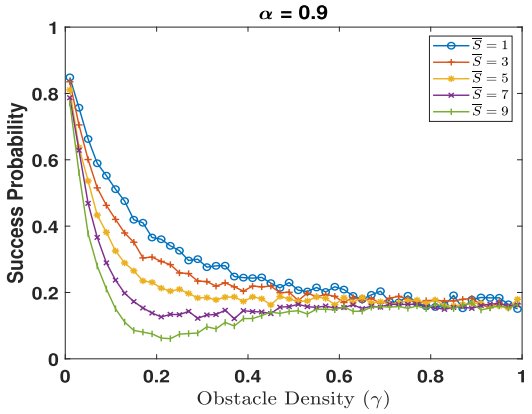

(a) Effect of Obstacle Density (γ) and Mean Speed $\{\overline{S}\}$ on Success Probability for $M = 5$

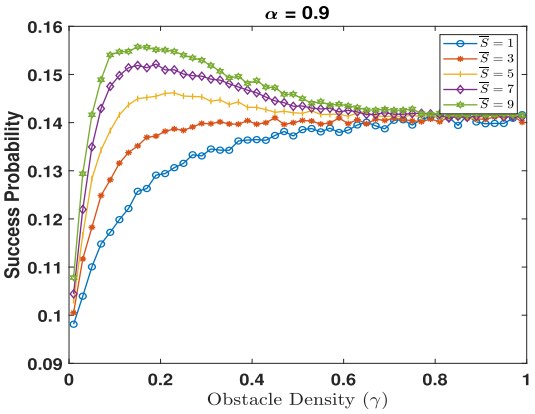

(b) Effect of Obstacle Density (γ) and Mean Speed $\overline{S}$ on Success Probability for $M = 150$

FIGURE 10. Success probability performance for $M = 5$ and $M = 150$.

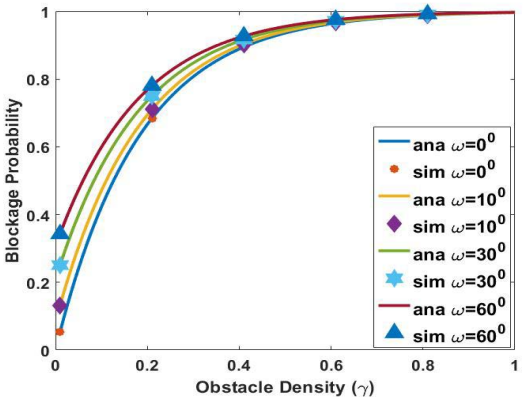

(a) Probability of blocking against the blockage density γ for a UE whose self-blockage angle is ω

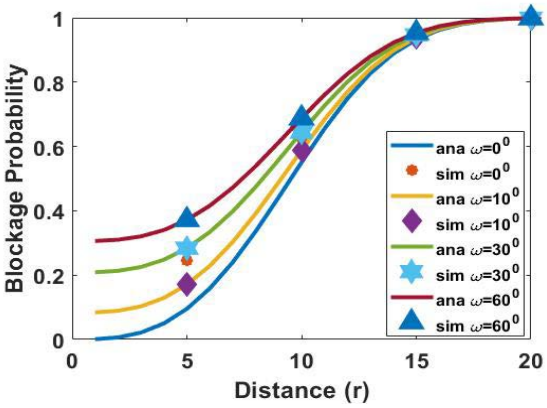

(b) Probability of blocking for a UE at a distance r for different self-blockage angle is ω

FIGURE 11. Effect of self-blockage on the NLoS probability.

the dependence of transmission of preambles solely depends on the coverage probability, hence the similar trends for Fig. 9b and 10a.

In Fig. 10b, for higher number of users ($M = 150$), we observe a rising trend in success probability with increasing obstacle density saturating at 14%, but is lower than 25% achieved in Fig. 10a. This is expected as the number of users increase the probability of transmission of same preamble increases, thus resulting into frequent collision. In Fig.10b, as the number of contending UEs are high, the success probability is very less even when obstacles are not present. At very low obstacle density, the success probability is low due to the large number of contending UEs. At that γ with the slight increase of obstacle density, many of the contending UEs can get blocked. Therefore the contention occurs only among the unblocked UEs and hence the success probability of the tagged UE increases. However, with the further increase in γ, the probability of the tagged UE getting blocked also increases and hence the success probability stars to decrease. The success probability gets saturated at the higher values of γ as the blockage probability of all UEs approaches and saturates to 1. We observed from Fig. 9b, the coverage probability decreases with increase in obstacle density, thus making the instances of beam failure and recovery more frequent. As the recovery instances increase and number of UEs are higher, the probability that multiple UEs recover the beam pair and transmit the same preamble increases. Thus resulting into decreased success probability.

Comparing Fig. 10a and 10b with the analytical results shown in Fig. 6a, we observe a similarity in trends observed thus confirming our analytical model with the simulations. Observing the simulation results, it can be seen that the average speed of UE has an effect on the coverage probability and the RACH success probability only in the lower range of obstacle densities.

IX. EFFECT OF SELF-BLOCKAGE

Self blockage occurs when the body of UE or the user holding the UE blocks a fraction of the viewing angle of the device [15], [31]. Let us denote the viewing angle blocked due to self-blockage is ω and the base stations that are shadowed by the user are no longer available for the UEs. If there are no base stations in the unshadowed region of a UE, then the UE is said to be in self-blockage condition. However, in this work, as our target is to analyze the random access success probability, we limit to the basestation (cell) at which the random access is performed. Hence the probability of the tagged base station being blocked due to the self blockage is given by $P_{self} = \omega/2\pi$. Thus the overall blockage probability of a UE at a distance r from the basestation considering the self blockage in conjunction with the blockage due to obstacles is denoted by $P_b^{ov}(r)$ and is given as follows.

$$\begin{aligned} P_b^{ov}(r) &= 1 - (1 - P_b(r))(1 - P_{self}) \\ &= 1 - exp\left(-\frac{\gamma r^3 \theta k}{\pi R}\right)\left(1 - \frac{\omega}{2\pi}\right) \end{aligned} \tag{32}$$

Figs. 11a and 11b show the effect of self blocking angle ω on the overall blockage probability of LoS path of the UE. The figures show that for a given distance of the UE from the base station r and a given obstacle density, the overall blockage probability increases with ω as supported by equation (32). The average blockage probability, P_b^{ov}, of a random UE can be calculated by averaging the above equation over the distribution of the distance of UE from the basestation.

$$\begin{aligned} P_b^{ov} &= \mathbb{E}_r[P_b^{ov}(r)] \\ &= \int_0^R \left(1 - exp\left(\left(-\frac{\gamma r^3 \theta k}{\pi R}\right)\left(1 - \frac{\omega}{2\pi}\right)\right)\right)\frac{2r}{R^2}dr \\ &= 1 + \left(\frac{2}{3}E_{\frac{1}{3}}\left(\frac{\gamma\theta k R^3}{\pi R}\right) - \frac{2}{3R^2}\frac{\Gamma(\frac{2}{3})}{(\frac{\gamma\theta k}{\pi R})^{2/3}}\right)\left(1 - \frac{\omega}{2\pi}\right) \end{aligned} \tag{33}$$

where $E_n(x)$ is defined in equation (16). Replacing $P_b(r)$ in equations (12), (13) and (22) with $P_b^{ov}(r)$ given equation (32) and evaluating the equation (24) gives us the coverage probability of a UE when self blockage is considered. Further, substituting the recalculated equation (24) in (27) gives the success probability of the random access procedure of a given UE.

X. CONCLUSION

In this paper we analytically derived the blockage probability of a UE using geometric and queuing theory techniques. Further, we have calculated the interference statistics of a UE in the cell considering the blockage, shadowing and the path loss effects closely following the 5G NR standard. The success probability of the random access procedure, which is a crucial step in connection establishment of a UE is calculated. We have performed extensive simulations to show the effect of mobility on the blockage probability, coverage probability and the success probability of the random access procedure. We have considered in our simulations that the UEs move in the cell according to the Gauss-Markov model to imitate the realistic UE movement. The simulation results are in good agreement with the analytical results derived in the paper validating out proposed model. The effect of mobility of UEs on their coverage probability and the RACH success probability has been evaluated in this paper. We have shown through simulations that the speed of UEs effect the RACH success probability differently depending on the number of competing UEs. In a nutshell, this work clearly established the relation between the cell environment along with the system configuration with the performance of random access procedure. For example, our results suggest that the number of preambles mapped to a RACH occasion in urban area network should be larger than that in the rural area deployments. Thus this work provides sufficient motivation and future direction to explore the adaptive basestation configurations like the number of available preambles, in turn the RACH configuration selection based on the network environment.

APPENDIX

A. PROBABILITY DISTRIBUTION OF S_1, S_2, S_3 AND S_4

As defined in Section V, S_1, S_2, S_3 and S_4 are the ratio of two independent lognormal random variables, not necessarily identical. In this appendix, we derive the general probability distribution of the ratio of two log normal random variables, which is used in calculating the interference power on a reference link. The end results are presented in V in the equations (17) and (18). Let X and Y are two independent lognormal (LN) random variables with the following parameters.

$$X \sim LN(\mu_1, \sigma_1^2), \quad Y \sim LN(\mu_2, \sigma_2^2) \tag{34}$$

As per the definition of log normal distribution, we construct two normal random variables as follows

$$\begin{aligned} X_N &= ln(X) \sim N(\mu_{1n}, \sigma_{1n}^2) \\ Y_N &= ln(Y) \sim N(\mu_{2n}, \sigma_{2n}^2) \end{aligned} \tag{35}$$

where the mean and variance of X_N and Y_N are given as follows.

$$\begin{aligned} \mu_{1n} &= 2ln(\mu_1) - \frac{1}{2}ln(\sigma_1^2, \mu_1^2) \\ \sigma_{1n}^2 &= -2ln(\mu_1) + ln(\sigma_1^2, \mu_1^2) \\ \mu_{2n} &= 2ln(\mu_2) - \frac{1}{2}ln(\sigma_2^2, \mu_2^2) \\ \sigma_{2n}^2 &= -2ln(\mu_2) + ln(\sigma_2^2, \mu_2^2) \end{aligned} \tag{36}$$

Since X and Y are independent, X_N and Y_N are also independent. Difference of the two normal distributions X_N and Y_N is denoted by another random variable $Z_N \sim N(\mu_{zn}, \sigma_{zn}^2)$ whose parameters are given as follows

$$\begin{aligned} \mu_{zn} &= \mu_{1n} - \mu_{2n} = ln\left[\left(\frac{\mu_1}{\mu_2}\right)^2\sqrt{\frac{\sigma_2^2 + \mu_2^2}{\sigma_1^2 + \mu_1^2}}\right] \\ \sigma_{zn}^2 &= \sigma_{1n}^2 + \sigma_{2n}^2 = ln\left[\frac{(\sigma_1^2 + \mu_1^2)(\sigma_2^2 + \mu_2^2)}{\mu_1^2\mu_2^2}\right] \end{aligned} \tag{37}$$

Now, we take exponential of Z_N to create a lognormal variable Z, which is the ratio of X and Y.

$$Z = e^{Z_N} = e^{X_N - Y_N} = e^{ln(X) - ln(Y)} = \frac{X}{Y} \tag{38}$$

The parameters of the probability distribution of Z is determined as follows.

$$\begin{aligned}\mu_z &= e^{\mu_{zn} + \frac{1}{2}\sigma_{zn}^2} = \frac{(\mu_2^2 + \sigma_2^2)\mu_1}{\mu_2^3} \\ \sigma_z^2 &= e^{2\mu_{zn} + \sigma_{zn}^2}(e^{\sigma_{zn}^2} - 1) \\ &= \left(\frac{\mu_1}{\mu_2}\right)^2 \left(1 + \frac{\sigma_2^2}{\mu_2^2}\right)^2 \left(\left(1 + \frac{\sigma_1^2}{\mu_1^2}\right)\left(1 + \frac{\sigma_2^2}{\mu_2^2}\right) - 1\right)\end{aligned} \tag{39}$$

This completes the derivation of the probability distribution of ratio of two log-normal random variables. The expected values of S_1, S_2, S_3 and S_4 are obtained by substituting appropriate μ_1, μ_2, σ_1 and σ_2 in 39 and are presented in (17) and (18) of Section V.

REFERENCES

[1] N. H. Mahmood *et al.*, "White paper on critical and massive machine type communication towards 6G," 2020, *arXiv:2004.14146*.
[2] *3GPP, Study on Channel Model for Frequencies From 0.5 to 100 GHZ (Release 16)*, Standard (TR) 38.901, Version 16.1.0, Tech. Rep., Nov. 2020.
[3] S. Rangan, T. S. Rappaport, and E. Erkip, "Millimeter-wave cellular wireless networks: Potentials and challenges," *Proc. IEEE*, vol. 102, no. 3, pp. 366–385, Feb. 2014.
[4] S. Tripathi, N. V. Sabu, A. K. Gupta, and H. S. Dhillon, "Millimeter-wave and terahertz spectrum for 6G wireless," 2021, *arXiv:2102.10267*.
[5] G. R. MacCartney, S. Deng, S. Sun, and T. S. Rappaport, "Millimeter-wave human blockage at 73 GHz with a simple double knife-edge diffraction model and extension for directional antennas," in *Proc. IEEE 84th Veh. Technol. Conf. (VTC-Fall)*, Sep. 2016, pp. 1–6.
[6] J. G. Andrews, S. Buzzi, W. Choi, S. V. Hanly, A. Lozano, A. C. Soong, and J. C. Zhang, "What will 5g be, "What will 5G be?" *IEEE J. Sel. Areas Commun.*, vol. 32, no. 6, pp. 1065–1082, Jun. 2014.
[7] M. Xiao, S. Mumtaz, Y. Huang, L. Dai, Y. Li, M. Matthaiou, G. K. Karagiannidis, E. Björnson, K. Yang, I. Chih-Lin, and A. Ghosh, "Millimeter wave communications for future mobile networks," *IEEE J. Sel. Areas Commun.*, vol. 35, no. 9, pp. 1909–1935, Sep. 2017.
[8] A. N. Uwaechia and N. M. Mahyuddin, "A comprehensive survey on millimeter wave communications for fifth-generation wireless networks: Feasibility and challenges," *IEEE Access*, vol. 8, pp. 62367–62414, 2020.
[9] J. G. Andrews, F. Baccelli, and R. K. Ganti, "A tractable approach to coverage and rate in cellular networks," *IEEE Trans. Commun.*, vol. 59, no. 11, pp. 3122–3134, Nov. 2011.
[10] M. Haenggi, *Stochastic Geometry for Wireless Networks*. Cambridge, U.K.: Cambridge Univ. Press, 2012.
[11] M. Di Renzo, "Stochastic geometry modeling and analysis of multi-tier millimeter wave cellular networks," *IEEE Trans. Wireless Commun.*, vol. 14, no. 9, pp. 5038–5057, Sep. 2015.
[12] A. K. Gupta, J. G. Andrews, and R. W. Heath, Jr., "Macrodiversity in cellular networks with random blockages," *IEEE Trans. Wireless Commun.*, vol. 17, no. 2, pp. 996–1010, Feb. 2018.
[13] M. K. Müller, M. Taranetz, and M. Rupp, "Analyzing wireless indoor communications by blockage models," *IEEE Access*, vol. 5, pp. 2172–2186, 2017.
[14] V. Raghavan, M.-L. C. Chi, M. A. Tassoudji, O. H. Koymen, and J. Li, "Antenna placement and performance tradeoffs with hand blockage in millimeter wave systems," *IEEE Trans. Commun.*, vol. 67, no. 4, pp. 3082–3096, Apr. 2019.
[15] V. Raghavan, L. Akhoondzadeh-Asl, V. Podshivalov, J. Hulten, M. A. Tassoudji, O. H. Koymen, A. Sampath, and J. Li, "Statistical blockage modeling and robustness of beamforming in millimeter-wave systems," *IEEE Trans. Microw. Theory Techn.*, vol. 67, no. 7, pp. 3010–3024, Jul. 2019.
[16] G. George, K. Venugopal, A. Lozano, and R. W. Heath, Jr., "Enclosed mmWave wearable networks: Feasibility and performance," *IEEE Trans. Wireless Commun.*, vol. 16, no. 4, pp. 2300–2313, Apr. 2017.
[17] S. Sun, T. S. Rappaport, S. Rangan, T. A. Thomas, A. Ghosh, I. Z. Kovacs, I. Rodriguez, O. Koymen, A. Partyka, and J. Jarvelainen, "Propagation path loss models for 5G urban Micro- and macro-cellular scenarios," in *Proc. IEEE 83rd Veh. Technol. Conf. (VTC Spring)*, May 2016, pp. 1–6.
[18] H. Tataria, K. Haneda, A. F. Molisch, M. Shafi, and F. Tufvesson, "Standardization of propagation models for terrestrial cellular systems: A historical perspective," *Int. J. Wireless Inf. Netw.*, vol. 28, no. 1, pp. 20–44, Mar. 2021.
[19] M. Giordani, M. Polese, A. Roy, D. Castor, and M. Zorzi, "A tutorial on beam management for 3GPP NR at mmWave frequencies," *IEEE Commun. Surveys Tuts.*, vol. 21, no. 1, pp. 173–196, 1st Quart., 2018.
[20] Y.-N.-R. Li, B. Gao, X. Zhang, and K. Huang, "Beam management in millimeter-wave communications for 5G and beyond," *IEEE Access*, vol. 8, pp. 13282–13293, 2020.
[21] F. Bai, N. Sadagopan, and A. Helmy, "The IMPORTANT framework for analyzing the impact of mobility on performance of RouTing protocols for Adhoc NeTworks," *Ad Hoc Netw.*, vol. 1, no. 4, pp. 383–403, 2003.
[22] M. J. F. Alenazi, S. O. Abbas, S. Almowuena, and M. Alsabaan, "RSSGM: Recurrent self-similar Gauss–Markov mobility model," *Electronics*, vol. 9, no. 12, p. 2089, Dec. 2020.
[23] S. Niknam, B. Natarajan, and R. Barazideh, "Interference analysis for finite-area 5G mmWave networks considering blockage effect," *IEEE Access*, vol. 6, pp. 23470–23479, 2018.
[24] K. Lyu, Z. Rezki, and M.-S. Alouini, "Accounting for blockage and shadowing at 60-GHz mmWave mesh networks: Interference matters," in *Proc. IEEE Int. Conf. Commun. (ICC)*, May 2018, pp. 1–6.
[25] T. Bai, R. Vaze, and R. W. Heath, Jr., "Analysis of blockage effects on urban cellular networks," *IEEE Trans. Wireless Commun.*, vol. 13, no. 9, pp. 5070–5083, Sep. 2014.
[26] C. A. Levis, "Friis free-space transmission formula," *Encyclopedia RF Microw. Eng.*, pp. 1733–1734, Apr. 2005, doi: 10.1002/0471654507.eme141.
[27] S. Singh, R. Mudumbai, and U. Madhow, "Interference analysis for highly directional 60-GHz mesh networks: The case for rethinking medium access control," *IEEE/ACM Trans. Netw.*, vol. 19, no. 5, pp. 1513–1527, Oct. 2011.
[28] J. Medhi, *Stochastic Processes*. Chennai, India: New Age International, 1994.
[29] G. K. Karagiannidis and A. S. Lioumpas, "An improved approximation for the Gaussian Q-function," *IEEE Commun. Lett.*, vol. 11, no. 8, pp. 644–646, Aug. 2007.
[30] Y. D. Beyene, R. Jäntti, and K. Ruttik, "Random access scheme for sporadic users in 5G," *IEEE Trans. Wireless Commun.*, vol. 16, no. 3, pp. 1823–1833, Mar. 2017.
[31] I. K. Jain, R. Kumar, and S. S. Panwar, "The impact of mobile blockers on millimeter wave cellular systems," *IEEE J. Sel. Areas Commun.*, vol. 37, no. 4, pp. 854–868, Apr. 2019.

LOKESH BOMMISETTY (Member, IEEE) received the Bachelor of Technology degree in electronics and communication engineering from the National Institute of Technology Goa, Goa, India, in 2017. He is currently pursuing the Ph.D. degree with the Indian Institute of Technology Madras, Chennai, India. His research interests include communication networks, scheduling, stochastic modeling, and performance evaluation of medium access layer in wireless networks.

SAGAR PAWAR received the bachelor's degree in electronics and telecommunications, in 2015, and the Master of Technology degree in communications and signal processing from the Indian Institute of Technology, Madras, India, in 2021. His research interests include signal processing, synchronization techniques, and preamble designs for wireless and random access procedures.

T. G. VENKATESH received the B.E. degree in electronics and instrumentation engineering from Annamalai University, India, in 1986, the M.E. degree in applied electronics from Bharathiar University, Coimbatore, India, in 1988, and the Ph.D. degree from the Indian Institute of Science, Bengaluru, India, in 1993. For a brief duration, he was with the Centre for Development of Telematics and the Indian Space Research Organization, Bengaluru. From 1994 to 1999, he was a Faculty Member with the Indian Institute of Technology, Delhi, India. He is currently a Faculty Member with the Electrical Engineering Department, Indian Institute of Technology, Madras, Chennai, India. His research group currently focuses on design and performance evaluation of medium access layer protocol in wireless networks and multicore architecture. He has authored a book on *Developing Multimedia Applications With the Java Media Framework* and coauthored the book *Computer Systems Design and Architecture*, published by Pearson. His research interests include stochastic modeling, computer networks, and computer architecture.